Investigations on the dynamic properties of 25,26,27,28-tetraalkoxycalix[4]arenes: *para*-substituent- and solvent-dependent properties of *paco* conformers and determination of thermodynamic parameters of the *pinched cone/pinched cone* conversion

Antonio Soi, Walter Bauer, Harald Mauser, Claus Moll, Frank Hampel and Andreas Hirsch *

Institut für Organische Chemie, Henkestr. 42, D-91054 Erlangen, Germany

The conformational and dynamic behaviour of the 25,26,27,28-tetraalkoxycalix[4]arenes 1–7 (R = methyl, propyl) has been investigated by X-ray crystallography, dynamic 1D and 2D NMR spectroscopy, as well as with a series of force field (PIMM) and semiempirical (PM3, MNDO) calculations. The stereo-electronic effects of the upper rim substituents of tetramethoxycalix[4]arenes characteristically influence the preferred arrangement of the phenyl rings in the *paco* conformation. The *in/out* isomerisation (0001~AAAA$\rightleftharpoons$0001~AAAB) taking place in 4 is strongly hindered in 1 due to the smaller diameter of the upper rim. The ease of rotation of the methoxy group attached to the inverted ring in *paco*-4 can be altered by using a solvent (CD_2Cl_2), which is able to form a host–guest complex with the calixarene cavity. For 1–3 *cone/paco* and *paco/paco* equilibria have been observed by 2D EXSY spectroscopy. Gibbs activation energies for the *cone*(C_{2v})/*cone*(C_{2v}) conversion were determined for 1, 2, 5 and 6. An NMR line shape analysis provided Arrhenius and Eyring activation parameters for the *cone*(C_{2v})/*cone*(C_{2v}) conversion in 5 and 6.

Introduction

Calixarenes[1–4] represent a class of compounds which is subject to intensive investigations in the field of supramolecular chemistry. The most simple representative of these macrocycles is 25,26,27,28-tetrahydroxycalix[4]arene. The four phenol type H-atoms form a ring of hydrogen bonds which stabilise the so called *cone* conformation. Early NMR studies[1] showed that the *cone* conformation is in dynamic equilibrium with its inverted conformation. Additional conformations, namely the partial *cone* (*paco*), the 1,2-*alternate* (1,2-*alt*) and the 1,3-*alternate* (1,3-*alt*) conformers are stabilized next to the *cone* (*co*), when the phenol type H-atoms are replaced by other substituents (Fig. 1).

In the case of the corresponding methyl and ethyl ethers these conformers are in dynamic equilibrium. When larger substituents are used, the conformations are fixed[5,6] and the corresponding calix[4]arenes can be separated, for example, by chromatography. The most prominent representative of the tetramethoxycalix[4]arenes is compound **4**[7] with *tert*-butyl substituents attached at the upper rim. In $CDCl_3$ solution at 243 K the ratio of the four conformers of **4** is 85.6% *paco*, 6.1% 1,2-*alt*, 5.5% *co* and 2.8% 1,3-*alt*.[8,9] The dynamic conversion of these conformers was investigated theoretically[8,10,11] as well as by NMR spectroscopy.[8,12,13] The ^1H NMR spectrum of the *cone* conformer of **4** is consistent with C_{4v}-symmetry. Molecular mechanics calculations, however, show that the lowest energy *cone* conformation has C_{2v}-symmetry (*pinched cone*). The ^1H NMR spectrum of **4** was explained with a rapid *co*(C_{2v})/*co*(C_{2v}) conversion.[14] We and others[8] could not observe the coalescence phenomenon in **4** upon cooling down to temperatures as low as 176 K (500 MHz). However, temperature dependent ^1H NMR investigations on 25,26,27,28-tetraoctyloxycalix[4]arenes with unsubstituted,[15] carboxy or aminocarbonyl substituted upper rims[16] gave unambiguous evidence for this very rapid interconversion. For example, for the aromatic protons of the parent tetramethoxycalix[4]arene a coalescence phenomenon at 188 K[17] was observed.

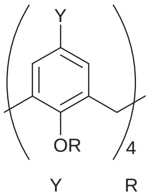

	Y	R
1	Br	Me
2	NO_2	Me
3	NH_2	Me
4	Bu^t	Me
5	NO_2	Pr^n
6	NH_2	Pr^n
7	Bu^t	Pr^n

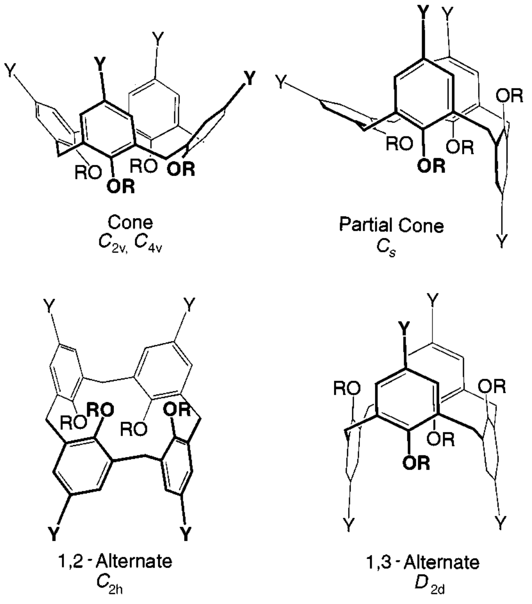

Fig. 1 The four possible conformers of tetraalkoxycalix[4]arenes

In a research project aimed at the synthesis of calixarene nanostructures and their supramolecular chemistry we synthesized the known compounds **1**–**7** as starting materials for the preparation of substituted biphenylcalix[4]arenes and peptido-

Table 1 PIMM calculated heats of formation (kcal mol^{-1}), strain energies with split terms (kcal mol^{-1}) and dipole moments (Debye) of **1**

Conformation	$\Delta_f H$	Strain energy	E_{Bond}	E_{Angles}	E_{Twist}	$E_{Bending}$	$E_{Coulomb}$	$E_{van\ d.\ Waals}$	Dipole moment
1									
0000~AAAA	−50.8	−42.8	0.2	3.6	2.6	0.9	−36.1	−14.1	4.00
0001~AAAA	−53.1	−44.3	0.1	2.5	3.3	0.7	−35.9	−15.0	2.13
0001~AAAB	−54.9	−45.9	0.2	3.3	3.5	0.6	−36.9	−16.5	2.80
0001~ABAA	−50.6	−36.6	0.4	4.6	10.5	1.2	−39.1	−14.2	2.67
0011~AAAA	−49.9	−42.9	0.2	3.2	2.1	0.4	−35.7	−13.3	0
0101~AAAA	−54.5	−44.5	0.1	1.7	3.6	0.8	−35.2	−15.7	0
1[a]									
0001′~AAAA	−55.5	−44.5	0.1	2.4	5.1	0.9	−37.2	−16	1.93
0001′~AAAB	−53.7	−44.0	0.3	3.2	6.9	0.6	−39.2	−15.9	2.08
0001′~ABAA	−47.7	−32.7	0.5	3.3	16.0	1.4	−39.2	−14.8	2.59

[a] Start geometry obtained from the X-ray structure. In all these calculated rotamers the proximal rings are slightly twisted.

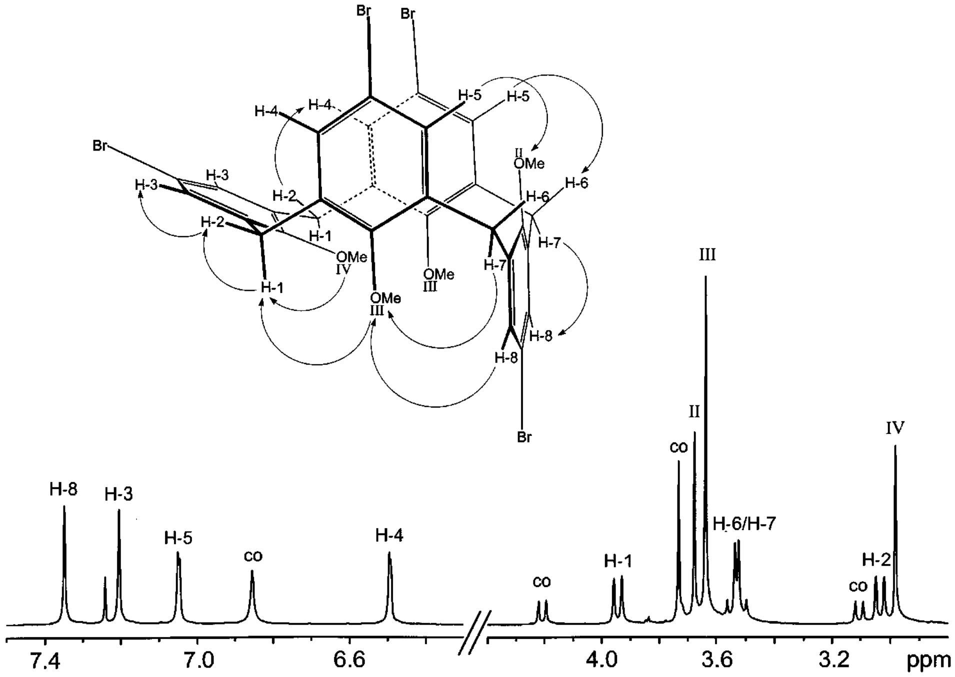

Fig. 2 NOE relationships and signal assignment of *paco*-**1** (CDCl$_3$, 238 K)

calix[4]arenes. During the spectroscopic characterisation of such derivatives we recognised that their dynamic behaviour in solution is closely related to that of the precursor compounds **1**–**7**. In order to get a closer insight into these phenomena we decided to use **1**–**7** as model compounds for a comprehensive and systematic investigation of their dynamic behaviour, by using both NMR spectroscopy and computational methods. We especially emphasise the influence of the stereo-electronic effects of the upper rim substituents as well as of the solvent on the conformational and dynamic behaviour of *paco* tetramethoxy[4]calixarenes using X-ray crystallography as well as temperature dependent and 2D NMR spectroscopy. We demonstrate once more that stereo-electronic effects of the substituents of the upper rim play an important role. Moreover, using tetramethoxycalix[4]arenes as model compounds, the three characteristic modes of conformational changes, namely: the *co*/*paco* equilibrium, the *co*(C_{2v})/*co*(C_{2v}) conversion and the rotation of the lower rim methoxy groups were investigated. For the corresponding tetrapropyloxycalix[4]arenes free Gibbs activation energies as well as Arrhenius and Eyring activation parameters were determined for the *co*(C_{2v})/*co*(C_{2v}) conversion.

Results and discussion

A. *paco* Conformations of tetramethoxycalix[4]arenes

The ^{1}H NMR spectrum of **1** in CDCl$_3$ or CD$_2$Cl$_2$ at room temperature shows the typical resonances[7] characteristic for the *cone* and the *paco* conformation. In CDCl$_3$ the ratio of *paco*:*cone* is 78%:22%. From a series of temperature dependent ^{1}H NMR spectra of **1** in CD$_2$Cl$_2$ a van't Hoff plot ($r = 0.97$) was generated giving $\Delta H° = -1.72 \pm 0.20$ kcal mol^{-1} and $\Delta S° = -5 \pm 1$ cal mol^{-1} K^{-1} for the equilibrium *co*$\rightleftharpoons$*paco* ($K = [paco]/[co]$). These numbers are very similar to those that have been reported by Shinkai and co-workers[8] for the related compound **4**, showing that in both cases the *paco*-conformer is the most stable. The calculated energy differences between the *paco* and the *cone* conformer are −2.3 kcal mol^{-1} (MNDO[18a]) and −2.1 kcal mol^{-1} (PIMM force field,[19] Table 1). The semi-empirical PM3[18b] method predicts the opposite order of stability (see Supplementary material, SUPPL. NO. 57368, 2 pp.†).

The ^{1}H NMR signals of the *cone* and the *paco* conformers (Fig. 2) were assigned based on their COSY, COLOC and ROESY spectra. Two anisole units in *paco*-**1** (C_s) are identical. The protons H-4 and H-5 appear as an AB-system with a ^4J coupling constant characteristic for aromatics (Fig. 2). The protons H-8 reveal NOE signals with the methoxy groups III and the AB system H-6/H-7. The H-8 protons must belong to

---

† For details of the Supplementary Publications Scheme see 'Instructions for Authors', *J. Chem. Soc., Perkin Trans. 2*, available *via* the RSC Web page (http://www.rsc.org/authors). The supplementary data is also available on the RSC's web server, at http://www.rsc.org/suppdata/perkin2/1998/1471.

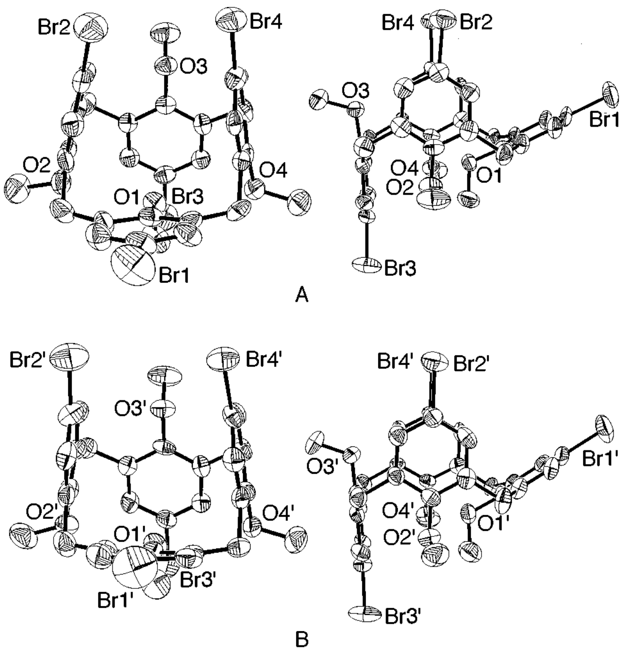

Fig. 3 X-ray crystal structure of *paco*-**1** showing the 0001′ conformer (A) and the 0001 conformer (B) from two different perspectives. Hydrogen atoms have been omitted for clarity.

the inverted ring, since the methoxy groups III producing one signal with double intensity belong to the identical anisole subunits. Therefore the AB-system H-6/H-7 must be due to CH_2-subunits connected to the inverted ring. The protons H-5 give rise to NOE-signals with the AB system H-6/H-7 and the methoxy group II. Therefore the methoxy group II must be bound to the inverted phenyl ring. The low field part of the AB system of the protons H-1/H-2 gives rise to NOE signals with the methoxy groups III, IV and to the high field part of the AB system. Therefore, the low field part corresponds to the *endo* protons (H-1) and the high field shifted methoxy group IV belongs to the anisole subunit located opposite to the inverted anisole ring. The ^{1}H NMR spectrum (CD_2Cl_2) of **2** is very similar to that of **1**. The signals of the H-6/H-7 methylene protons of *paco*-**2** are closely overlapping with those of the methoxy groups II and III. The ROESY spectrum of *paco*-**2** shows the same NOE relationships as observed for *paco*-**1**. Therefore, it can be concluded that the conformational characteristics of the *paco* forms of **1** and **2** are closely related, especially since in both cases the methoxy groups IV are the most high field shifted. A significantly different situation is deduced from the NOESY spectrum of compound **4**, recorded at 213 K in $CDCl_3$. From the cross peaks the following NOE relationships can be deduced: the most downfield shifted aromatic protons show a NOE signal with the methoxy groups III. These must be the H-8-protons of the inverted ring. The H-8-protons show also a NOE signal with a methylene AB-system which must be the H-6/H-7 protons. This AB-system gives also rise to a NOE signal with the high field shifted methoxy group II ($\delta = 1.8$). Therefore, in contrast to *paco*-**1** and *paco*-**2** the most high field shifted methoxy group is bound to the inverted ring.

The same peak assignment of *paco*-**4** was deduced by Shinkai and co-workers.[8] Hence, depending on the nature of the upper rim substituent the most high field shifted methoxy group in the *paco* form of tetramethoxycalix[4]arenes can either be the methoxy group II bound to the inverted anisole ring or the methoxy group IV. Unfortunately, the assignment for the corresponding methoxy group in *paco*-**3** was not possible due to the presence of overlapping resonances and the lack of NOE signals for the most high field shifted methoxy group. However, since both *paco*-**3** and *paco*-**4** gives rise to a similar temperature dependence (*vide infra*) of the high field shifted methoxy groups we believe that they adopt comparable conformations.

Single crystals of **1** suitable for X-ray crystallography were obtained from a DMSO solution. In the crystal **1** adopts the *paco* 0001~AAAA conformation[20] (Fig. 3). In the unit cell two independent molecules are found. In contrast to the experimental structure of *paco*-**4**[2] in both 0001~AAAA conformers of **1** the upper rim substituents of the proximal rings point towards each other, causing a significant contraction of the upper rim as compared to **4**. In one of these 0001~AAAA conformers the arrangement of the proximal bromine substituents is not strictly eclipsed but slightly staggered which causes the corresponding anisole rings to be twisted (Fig. 3). We denote this conformation with the smallest upper rim diameter as 0001′ conformation (*t* = twist).

The twisting of the anisole subunits and the contraction of the upper rim cavity is not reproduced by free geometry optimization using either the PIMM force field or the semiempirical PM3 and MNDO methods. In the calculated structures the proximal anisole rings are oriented almost parallel to each other. The orientation of the distal anisole rings on the other hand comes closer to the experimental structure. Interestingly, the PIMM minimization using the X-ray structure as starting geometry reproduces satisfactorily the experimental 0001′-structure. Moreover, the calculated heat of formation of the 0001′~AAAA structure obtained from the experimental starting geometry is 2.4 kcal mol^{-1} lower than for the corresponding 'normal' 0001~AAAA structure (Table 1). The twisting of the proximal rings in the X-ray structure can be rationalised in terms of energy gain due to attractive van der Waals and Coulomb interactions (Table 1). PM3 and MNDO minimizations starting with the experimental structure of **1** do not reproduce these results but lead to the same structures as those obtained from the free geometry optimizations (*vide supra*).

Dynamic behaviour of the methoxy groups. It is reasonable to assume that in the preferred conformation of *paco*-**1** in solution the proximal rings are similarly arranged as in the solid state 0001′ structure. This arrangement causes the diameter of the lower rim to increase and the diameter of the upper rim to decrease. As a consequence, the lower rim cavity should become more accessible for methoxy group IV whereas the decreased size of the upper rim makes the cavity less accessible for the methoxy group II.

Compared to the ^{1}H NMR chemical shift ($\delta = 3.78$) of the methoxy protons within free anisole the signals of methoxy group IV of *paco*-**1** appear with a high field shift of about $\delta = 0.8$. This high field shift is due to the influences of ring currents produced by the two proximal and the inverted anisole rings. An estimation of the influences of these ring currents using the anisotropy model of Johnson and Bovey[21] was carried out on the basis of the PM3 structure[22] of *paco*-**1** (ABAA). In this calculated conformation the methoxy group IV lies almost directly above the plane of the inverted anisole ring. The distance of the centre of the trigon determined by the three protons of the methoxy group from the centre of the inverted anisole ring is 3.22 Å. If one considers in a first approximation only the shielding of the inverted ring, a high field shift of approximately $\Delta\delta = 1.1$ can be expected. However, the two proximal rings are expected to give rise to an additional shielding of about $\delta = 0.85$ per ring. Hence, one would expect that the protons of the methoxy group IV in this conformer resonate at about $\delta = 1$. On the other hand for the fixed 0001~AAAA conformation a chemical shift of $\delta = 3.8$ can be assumed. With these estimations of the chemical shifts one can calculate the populations of these two states taking the experimental value $\delta = 3$. The *in*:*out* ratio is 0.4 at 298 K. As a consequence the energy difference ΔE between the two states is estimated to be 0.5 kcal mol^{-1}. Reinhoudt and co-workers[10] calculated a ΔE of 1.1 kcal mol^{-1} for the two conformers **4** 0001~AAAA and **4** 0001~ABAA (more stable) corresponding to an *in*:*out* ratio of 6.4 ($T = 298$ K). Upon cooling down to up to 176 K no coalescence phenomenon or broadening of the signals of methoxy group IV was observed. Therefore, we conclude that due to the increase of the lower rim diameter in *paco*-**1** the rotational barrier between the two states is very low.

The significant high field shift of methoxy group II observed in *paco*-**4** (*vide supra*) is absent in *paco*-**1**. This implies that the **1** 0001~AAAB conformation where the methoxy group II is exposed to the shielding of the two proximal rings is much less populated than the **1** 0001~AAAA conformation. Due to the sterically demanding *tert*-butyl groups the diameter of the upper rim in **4** is larger than that of **1**. This facilitates the rotation of methoxy group II and therefore increases its probability to be located within the cavity. The *out*/*in* isomerisation (0001~AAAA$\rightleftharpoons$0001~AAAB) in **4** can be considered as an exothermic process since during this process the self-complexation enthalpy[14] is released. This interpretation is also corroborated by the comparison of temperature dependent NMR spectra of **1**, **2**, **3** and **4**. Whereas the ^{1}H NMR signals of the most high field shifted methoxy group IV in **1** and **2** are independent of the temperature, the most high field shifted methoxy groups II of compounds **3** and **4** show a pronounced temperature dependence of up to 0.7 ppm between 304 and 218 K for **4** in $CDCl_3$. This temperature dependence of the methoxy group II in *paco*-**4** (and *paco*-**3**) can be explained in the following way: decreasing the temperature shifts the exothermic *out*/*in* isomerisation 0001~AAAA$\rightleftharpoons$0001~AAAB to the product side causing an increase of the population of methoxy groups inside the cavity which are exposed to the strong shielding of the two proximal anisoles. The rotation of the methoxy group II takes place but is hindered in the temperature range investigated. On the other hand the rotational barrier for the rotation of the methoxy group II (0001~AAAA$\rightleftharpoons$0001~AAAB) in **1** should be significantly higher because in this case, to enter the upper rim it would be necessary to overcome the attractive Coulomb and van der Waals interactions (Table 1). Therefore, due to the contraction of the upper rim the rotation of methoxy group II in *paco*-**1** and *paco*-**2** is strongly hindered. These findings reveal that the dynamic behaviour of the methoxy groups attached to the lower rim strongly depends on the preferred conformation (0001 or for example 0001^r) of the entire *paco* molecule. The overall dynamic behaviour of *paco*-conformers is strongly determined by the stereo-electronic properties of the upper rim substituents.

The dynamic behaviour of **4** changes dramatically when CD_2Cl_2 is used as solvent. Whereas in $CDCl_3$ solution the equilibrium *co*$\rightleftharpoons$*paco* is exothermic ($\Delta H^\circ = -1.9$ kcal mol^{-1} and $\Delta S^\circ = -2.4$ cal mol^{-1} K^{-1}) as reported by Shinkai and coworkers[8] we determined from the van't Hoff plot ($r = 0.98$) for the corresponding *co*/*paco* interconversion in CD_2Cl_2 a ΔH° of 1.35 ± 0.08 kcal mol^{-1} and a ΔS° of 8.07 ± 0.38 cal mol^{-1} K^{-1}. Similar values were reported by Reinhoudt *et al.*[23] Therefore, in $CDCl_3$ results show that the *co*/*paco* equilibrium is enthalpy controlled whereas in CD_2Cl_2 it is entropy controlled. This is a consequence of the ability of *cone*-**4**[11] to form a host–guest complex with CD_2Cl_2. In both solvents the *paco*-conformation is favoured. Another interesting behaviour of *paco*-**4** in CD_2Cl_2 is the temperature dependence of the most high field shifted methoxy group II ($\delta = 2.63$ at 273 K). Upon cooling the signal broadens and finally disappears at 178 K. Although the analysis of the NOESY spectrum did not allow for an unambiguous assignment of this methoxy group we assume that in both solvents $CDCl_3$ and CD_2Cl_2 the most high field shifted signal belongs to methoxy group II in *paco*-**4**. From the observation that in CD_2Cl_2 the methoxy group II resonates at lower field and also from the fact that it shifts to lower field with decreasing temperature we conclude that in CD_2Cl_2 the 0001~AAAA state is more populated than the 0001~AAAB state. The fact that the signal disappears indicates a coalescence phenomenon. It can be assumed that the barrier for the *in*/*out* isomerisation of the methoxy group II is higher in CD_2Cl_2 than in $CDCl_3$. We explain this in the following way: in $CDCl_3$ no complexation of the solvent takes place,[11] in this case only the *co*/*paco* interconversion equilibrium (1) and the self complexing equilibrium[14] (3) of the methoxy group II have to be considered. In CD_2Cl_2 the solvent S can be complexed by the cavity[11] and is therefore involved in the conformational equilibrium. As a consequence a series of coupled equilibria (1)–(4) has to be

$$co \rightleftharpoons paco \qquad (1)$$

$$co + \mathrm{S} \rightleftharpoons [co]^*\mathrm{S} \qquad (2)$$

$$\mathrm{0001{\sim}AAAB} \rightleftharpoons \mathrm{0001{\sim}AAAA} \qquad (3)$$

$$\mathrm{0001{\sim}AAAA} + \mathrm{S} \rightleftharpoons [\mathrm{0001{\sim}AAAA}]^*\mathrm{S} \qquad (4)$$

$$\mathrm{0001{\sim}AAAB} + \mathrm{S} \rightleftharpoons [\mathrm{0001{\sim}AAAA}]^*\mathrm{S} = (5) = (3) + (4)$$

taken into account considering that in addition to *cone*-**4**[11] also *paco*-**4** is able to incorporate a CD_2Cl_2 molecule.

Eqn. (4) shows how the rotamer equilibrium (3) is shifted towards the *out* conformation and therefore accounts for the lower population of the conformer 0001~AAAB. Eqn. (5) represents the overall rotational process involving the solvent and accounts for the higher rotational barrier in CD_2Cl_2 because here an *out*/*in* rotation is accompanied by the loss of a tightly bounded solvent molecule.[24] Assuming an equal population of the *in* and *out* rotamers and a lower and upper limit for the peak separation at 40 and 280 Hz, respectively, the free Gibbs activation enthalpy can be estimated to be in the range of 7.9–8.6 kcal mol^{-1}. This is in good agreement with $\Delta E^\ddagger = 10.7$ kcal mol^{-1} predicted for the methoxy rotation in 1,2-*alt*-**4** and 1,3-*alt*-**4**.[10]

Conformational interconversion of tetramethoxycalix[4]-arenes. Another dynamic phenomenon that we studied with compounds **1**–**3** is the so-called *paco*/*paco* conversion.[9,19] This conversion proceeds *via* the corresponding 1,3-*alt* conformations (fast) and the 1,2-*alt* conformations (slow).[9,13] In order to find out whether this dynamic phenomenon is a general process or whether it is restricted to compound **4** we carried out a series of 2D EXSY NMR investigations. The 2D EXSY spectrum of **1** (Fig. 4) recorded in $CDCl_3$ at 297 K shows a *cone*/*paco* conversion, which can be deduced from the position of the cross peaks. The *cone* H_{endo} exchanges with the *paco* H_{endo} and with the AB-system H-6/H-7. The exchange of the H_{exo} protons proceeds similarly. This indicates that during the *cone*/*paco* conversion the rotation of only one phenyl ring is involved.[8] The analysis of the aromatic region reveals that next to a *co*/*paco* exchange a *paco*/*paco* exchange is present. At 263 K (CD_2Cl_2) the *co*/*paco* exchange is significantly slower. Whereas for mixing times smaller than 0.4 s only cross-peaks between the *paco* signals are present, *cone*/*paco* cross-peaks appear again at a mixing time of 0.4 s. Therefore, the *paco*/*paco* exchange is faster than the *cone*/*paco* exchange. Since in the EXSY spectrum of **1** no cross-peaks between the *paco*-signals and the signals of the 1,2-*alt* and/or the 1,3-*alt* conformation are observed, it can be concluded that these conformers are either not present in detectable amounts or represent very short lived species. A *cone*/*paco* exchange was also observed for compound **2** (mixing time of 0.4 s, $T = 296$ K, CD_2Cl_2). In analogy to **4**,[9,13] we assume that the *paco*/*paco* conversion proceeds *via* the *alternate* conformations. A *paco*/*paco* conversion and simultaneous rotation of all anisole units at low temperatures should be excluded due to the high energy barrier expected for a simultaneous rotation of several anisole rings. For compound **3** the 1,2-*alt* conformation could be detected. In the ^{1}H–^{1}H-COSY NMR spectrum ([$^2H_7$]DMF, 213 K) four AB-systems can be clearly identified. Two of these AB-systems are attributed to the *paco*-**3** and one to the *cone* conformation. The remaining AB-system is due to the diastereotopic CH_2-unit of the 1,2-*alt* conformation. The singlet of the homotopic CH_2-unit is

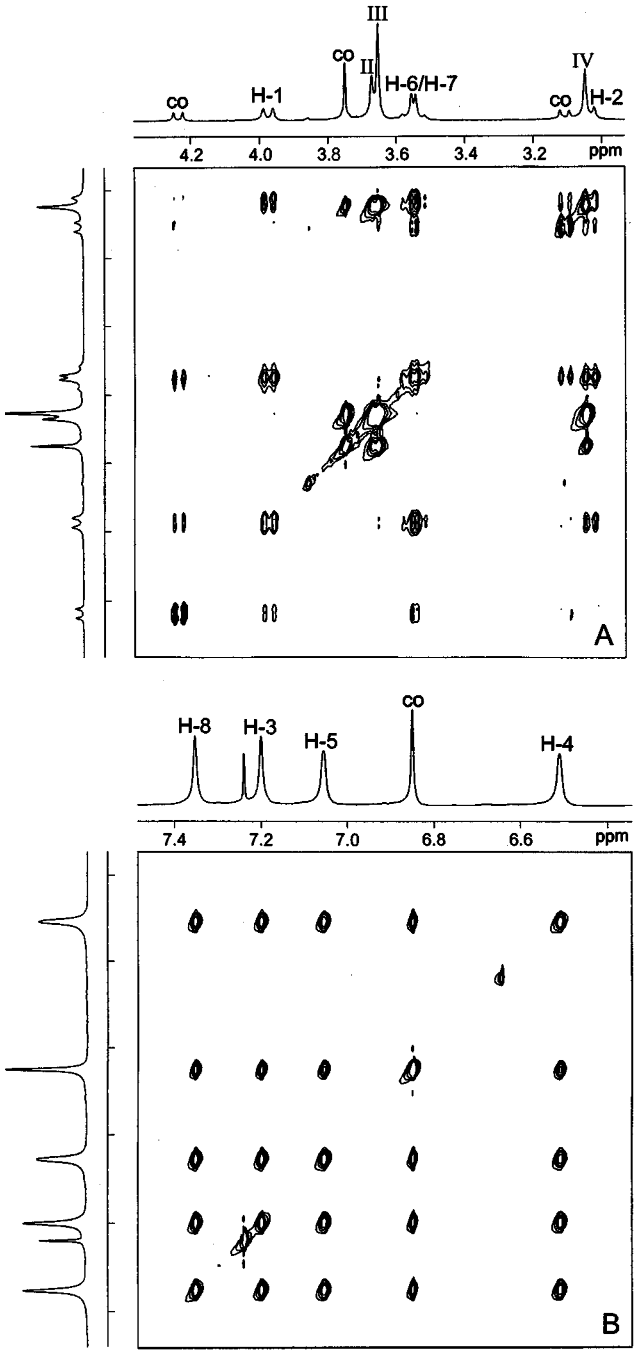

Fig. 4 2D EXSY spectrum (500 MHz, $CDCl_3$, RT, mixing time 0.4 s) of **1** showing the exchange signals between the *paco* and the *co* conformers. A, aliphatic region; B, aromatic region (for the labelling of the signals see also Fig. 2).

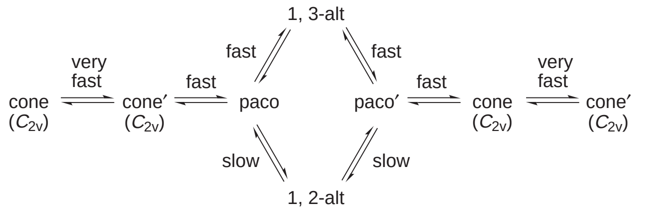

Fig. 5 Schematical representation of the interconversion equilibria between the different conformations of tetramethoxycalix[4]arenes. A quantitative analysis for the example of **4** is given by Blixt and Detellier.[13]

Table 2 Experimental coalescence temperatures, peak separations ($\Delta\delta$) of the aromatic protons, rate constants and free activation enthalpies for the *pinched cone*/*pinched cone* conversion in CD_2Cl_2

Compound	T_c/K	$\Delta\delta$/Hz	k_c/s^{-1}	$\Delta G^\ddagger$/kcal mol^{-1}
1	191[a]	265	588.3	8.6
2	223[a]	466	1034.5	9.8
5	233[b]	538.6	1195.8	10.2
6	185[b]	293	650.5	8.3

[a] 500 MHz. [b] 400 MHz.

covered by the methoxy signals of **3** *cone* at $\delta = 3.64$ which can be concluded from the ^1H–^{13}C COSY spectrum. The two aromatic protons of the 1,2-*alt* conformation give rise to one singlet at $\delta = 6.43$ showing a NOE signal with the high field part of the CH_2-AB-system and one signal which is covered by the resonance of the aromatic protons of the *cone* conformation. The latter signal shows a NOE with the homotopic CH_2-units and with the methoxy group at $\delta = 3.84$ (213 K, [$^2H_7$]DMF). From the integration of the Ar–H-signals a composition of the conformers *cone*:*paco*:1,2-*alt* of 40%:50%:10% ([$^2H_7$]DMF, 213 K) can be deduced. Whereas in the ROESY-spectrum of **3** exchange signals between the *cone* and the *paco* conformation (mixing time 0.05 s, 233 K) are detected and the same situation is revealed for the *paco*/*paco* exchange, the participation of the 1,2-*alt* conformation at the conformational exchanges can only be seen at a mixing time of 0.2 s (233 K). This result indicates that those conformational exchanges, in which the 1,2-*alt* conformation participates, proceed significantly slower, meaning that the *paco*/*paco* conversion in **3** proceeds fast *via* the 1,3-*alt* conformation and slow *via* the 1,2-*alt* conformation. These results are similar to those which have been already reported for compound **4**.[9,13] Therefore, it is reasonable to assume that the conformational exchanges of the tetramethoxycalix[4]arenes shown in Fig. 5 are of general validity. This is also implied by the MM3 calculations of Thondorf *et al.*[25] who showed that the ring inversion of *exo*-calix[4]arene and of 4-*tert*-butylcalix[4]arene proceeds also *via* a *paco* and 1,2-*alt* intermediate.

B. The C_{2v} cone/C_{2v} cone interconversion in tetraalkoxycalix[4]arenes[15–17,26,27]

Upon successive cooling of **1** in CD_2Cl_2 a broadening of the Ar–H and the methoxy signals of the *cone* conformer is observed. The singlet of the AR–H-protons shows a coalescence at 191 K and gives rise to two singlets at 176 K (Fig. 6). This coalescence phenomenon is due to the *cone*(C_{2v})/*cone*(C_{2v}) conversion. Out of the peak distance of these signals a $\Delta G^\ddagger$ of 8.6 kcal mol^{-1} was determined (Table 2).[28] The exact position of the new methoxy signals cannot precisely be determined, since these signals are still broad at 176 K and are partly covered by the signals of the *paco* conformation.

Unambiguous proof for the C_{2v}/C_{2v} conversion is provided by the ROESY spectrum of **2** recorded at 178 K. Only the exchange signals between the *pinched-cone* Ar–H-resonances and the methoxy resonances can be detected. The absence of *co*/*paco* and *paco*/*paco* cross-peaks indicates that the *pinched cone*/*pinched cone* conversion is the fastest mode of all macrocyclic motions within the tetramethoxycalix[4]arenes (Fig. 5). Similar investigations with **2** reveal a coalescence of the C_{2v}/C_{2v}-conversion at 223 K. Below the coalescence temperature the Ar–H-protons of the *pinched cone* conformation are covered by two of the *paco* signals.

The *cone* conformation of calix[4]arene **5** is fixed due to the introduction of four propyl substituents in the lower rim. Since in the ^1H NMR spectrum of **5** no signal overlap is present, favourable conditions for the deduction of activation parameters *via* line shape analysis are provided (Fig. 7). The line-shape analysis allows the determination of *k*-values and therefore, from the corresponding Arrhenius plot of ($r = 0.99$) the activation energy $E_A = 9.89 \pm 0.17$ kcal mol^{-1} and the frequency factor $A \approx 2.89 \times 10^{12}$ s^{-1}. From the Eyring plot ($r = 0.99$) an activation enthalpy $\Delta H^\ddagger = 9.42 \pm 0.17$ kcal mol^{-1} and an activation entropy $\Delta S^\ddagger = -3.07 \pm 0.74$ cal mol^{-1} K^{-1} are deduced.[29]

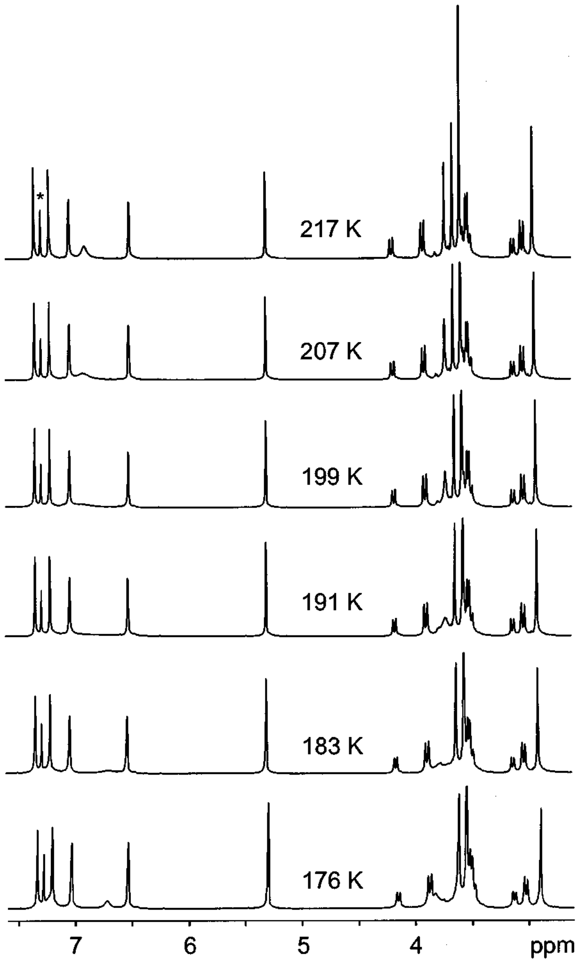

Fig. 6 Temperature dependent ^{1}H NMR spectra (500 MHz, CD_2Cl_2) of **1** (* = $CHCl_3$)

Table 3 PM3 activation enthalpies for the *pinched cone*/*pinched cone* conversion

Compound	Δ_fH ground state C_{2v}/ kcal mol^{-1}	Δ_fH transition state C_{4v}/ kcal mol^{-1}	$\Delta H^\ddagger$/ kcal mol^{-1}
1	−15.2	−14.2	0.8
2	−78.6	−77.3	1.3
3	−52.7	−51.2	1.6
4	−142.2	See text	See text

The value for $\Delta S^\ddagger$ is about twice the calculated value, taking into account only the change of the symmetry numbers as contribution to the activation entropy ($\Delta S^\ddagger = -R \ln 2 = -1.37$ cal mol^{-1} K^{-1}). Obviously, this process is accompanied only by minor changes within the solvent shell. The corresponding $\Delta H^\ddagger$ values calculated semiempirically (PM3) are presented in Table 3. These activation enthalpies are underestimated[30] by a factor of about 9. Nevertheless, the exact analysis of the calculated reaction coordinates shows that the calculations reflect the physical situation in the correct way.

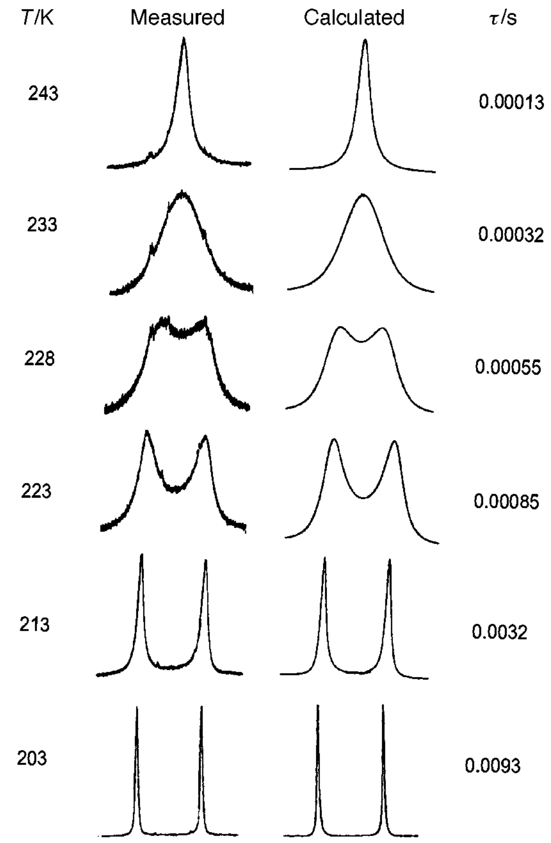

Fig. 7 Line shape analysis of the temperature dependent ^{1}H NMR spectra (400 MHz, CD_2Cl_2) of **5**. Calculated and measured signals of the aromatic protons.

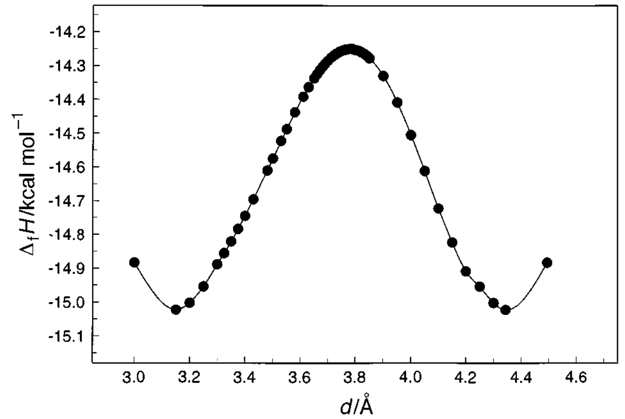

Fig. 8 PM3 calculated reaction coordinate for the *pinched cone*/*pinched cone* interconversion for the example of **1**

For compounds **1**, **2**, **3**, **5** and **6** a double minimum potential was established. Fig. 8 shows the reaction coordinate at the example of **1**. For the three extrema, namely the two minima and the saddle point, frequency calculations were carried out. The minima of the coordinate indeed correspond to minimum structures since the number of negative frequencies with C_{2v}-symmetry is zero. The saddle point structure exhibits a negative frequency and therefore corresponds to a C_{4v}-symmetrical transition state. The negative frequency is due to the lowest excitable normal frequency, which according to the calculation is Raman active like the lowest excitable normal frequency of the minimum structures. As can be seen from the corresponding frequency pictures (Fig. 9) both normal frequencies correspond to the same mode of motion of the molecule: the proximal anisole subunits are moving away from each other and at the same time the distal anisole units are moving towards each other. The reaction coordinate, which describes the *pinched cone*/*pinched cone* interconversion is therefore nothing else but the normal mode mentioned above. This is further corroborated by the fact that the frequency which corresponds to this normal mode is of the same order of magnitude as the frequency factor which was determined from the experimental data of compound **5**.

For compounds **4** and **7** in CD_2Cl_2 no coalescence was observed at temperatures as low as 173 K. The same is found for compound **3** ([$^2H_7$]DMF/CD_2Cl_2) but for the corresponding propyl ether **6** coalescence is reached at $T_c = 185.5$ K (400 MHz). With a peak separation of 293 Hz a $\Delta G^\ddagger$ of 8.3 kcal

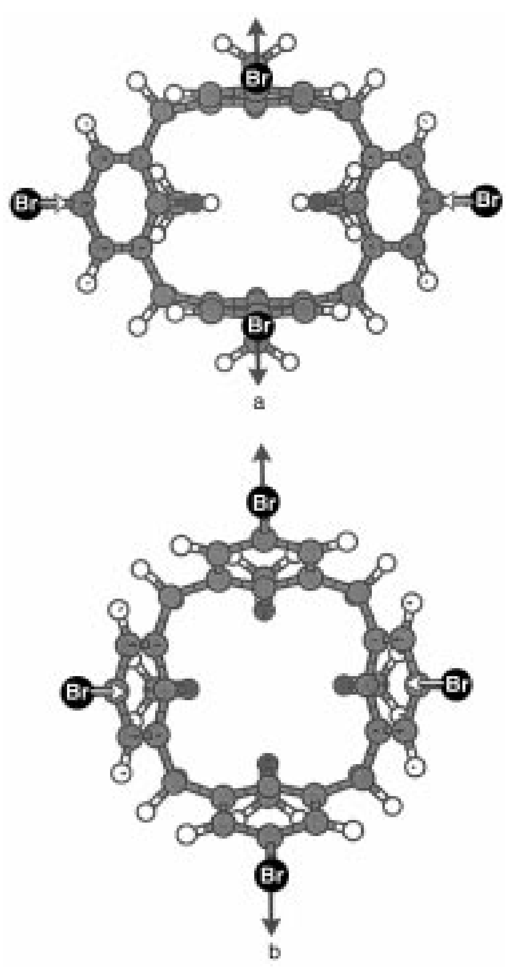

Fig. 9 PM3 geometries of *cone*-1 (a) C_{2v} ground state and (*b*) C_{4v} transition state. The arrows indicate the normal mode and the imaginary frequency, respectively.

mol^{-1} is calculated at the coalescence temperature. The Eyring plot ($r = 0.90$) obtained from the line shape analysis allows us to deduce the $\Delta G^{\ddagger}$ with $\Delta H^{\ddagger} = 4.71 \pm 0.37$ kcal mol^{-1} and $\Delta S^{\ddagger} = -19.33 \pm 1.74$ cal mol^{-1} K^{-1}. We believe that the high negative magnitude of $\Delta S^{\ddagger}$ is due to a solvation effect.[31] The transition state seems to be more strongly solvated then the ground state and as a consequence the C_{2v}/C_{2v} conversion is accompanied by a solvent ordering process. The relative stabilisation of the transition state by solvation decreases the energy barrier for the interconversion process and therefore accounts for the smaller $\Delta H^{\ddagger}$ value compared with that of compound **5**. The stabilisation of the C_{4v} transition state compared to the C_{2v} ground state is probably due to more effective intermolecular hydrogen bonding in the more symmetrical transition structure.

For compound **4** an energy barrier for the C_{2v}/C_{2v} conversion of 5.1 kcal mol^{-1} was calculated for the case where a CD_2Cl_2 molecule is incorporated within the cavity[11] (and a barrier of 3.2 kcal mol^{-1} for an empty cavity).[14] If one assumes a chemical shift difference for the Ar–H protons of 390 Hz (mean value of the numbers presented in Table 2), then a coalescence temperature $T_c = 117$ K is to be expected if a 500 MHz spectrometer is used. It is clear that these conditions are hard to achieve experimentally. The semiempirical calculation (PM3) of the reaction coordinate for compound **4** shows that the C_{2v}/C_{2v} conversion in contrast to those of **1**, **2** and **3** does not proceed *via* a C_{4v} symmetrical transition state, but a C_{4v}-*cone* intermediate. The *para* C-atoms (upper rim) of the C_{2v} ground state ($\Delta H^{\circ} = -142.2$ kcal mol^{-1}) are located in the middle of the edge of a rectangle of length $l = 9.1$ Å and width $b = 5.3$ Å. During the conversion the molecule approaches a C_{2v}-symmetrical transition state ($\Delta H^{\circ} = -138.3$ kcal mol^{-1}), where the length of the rectangle is reduced to $l = 7.3$ Å and the width is enlarged to $b = 6.0$ Å. Whereas the length of the rectangle ($b = 7.3$ Å) is not very much affected, the width is further enlarged ($b = 7.3$ Å) within the local minimum structure ($\Delta H^{\circ} = -140.2$ kcal mol^{-1}) of the intermediate. With $\Delta H^{\ddagger} = 3.9$ kcal mol^{-1} and $\Delta S^{\ddagger} = -3.07$ cal mol^{-1} K^{-1} and taking into account the shift difference of the two signals of $\delta = 390$ a coalescence temperature $T_c = 92$ K is to be expected with a 500 MHz spectrometer. This estimated coalescence temperature represents a lower limit, since as mentioned above, the calculated activation energies are significantly underestimated. Upon cooling down solutions of the *cone* conformers of **4** and **7** one would expect three instead of two signals for the aromatic protons after passing the coalescence temperature. One signal would correspond to the C_{4v}-*cone* and the other two to the *pinched cone* conformation. The introduction of a *tert*-butyl group to the upper rim obviously lowers the energy of the C_{4v}-*cone* structure. Therefore, in contrast to compounds **1**, **2**, **3**, **5** and **6** the C_{4v}-*cone* structure is no longer a transition state but an intermediate which exists in an equilibrium with the *pinched cone* conformers.

Conclusions

With tetramethoxycalix[4]arenes **1**–**4** as model compounds, we investigated the three characteristic modes of conformational changes, namely the *cone*/*paco* equilibrium, the *cone*(C_{2v})/*cone*(C_{2v}) conversion and the rotation of the methoxy groups of the lower rim. These conformational motions within tetramethoxy[4]calixarene seem to be general and are not to be restricted to the examples reported so far in the literature. The dynamics of these motions strongly depend on the nature of the upper rim substituents. In the case of the tetrabromo derivative **1**, the X-ray single crystal structure reveals a *paco* 0001′~AAAA conformation, where the upper rim is significantly contracted compared to **4**. As a consequence, in **1** the 0001~AAAB conformation is less preferred. This causes completely different temperature dependent NMR spectra for **1** and **4**. From the comparison of the NMR spectroscopic behaviour it can be concluded that the tetranitro derivative **2** behaves like **1**, whereas the tetraamino derivative **3** behaves like **4**. The preferred *paco* conformation of **4** changes from 0001~AAAB in $CDCl_3$ to 0001~AAAA in CD_2Cl_2. This is due to the formation of a host–guest complex between *paco*-**4** with the smaller solvent molecule CD_2Cl_2 which blocks the calixarene cavity and disfavours a facile rotation of the methoxy group of the inverted ring. In line with these findings is the observation that the nonpreference of the 0001~AAAB conformation within *paco*-**1** is observed in both solvents, $CDCl_3$ and CD_2Cl_2. The contraction of the upper rim perimeter prevents also the smaller CD_2Cl_2-guest from a facile complex formation with the calixarene cavity. This consolidation and extension of the existing knowledge about calix[4]arenes could be very useful for further studies in the field of supramolecular calixarene chemistry as well as for the tailor design of calixarene-nanostructures. Work along these lines is currently underway.

Experimental

^{1}H NMR and ^{13}C NMR: JEOL JNM GX 400 and JEOL ALPHA 500. Compounds **1**–**7** were synthesised according to literature procedures: **1**,[32] **2**,[33] **3**,[34] **4**,[7] **5**,[33] **6**,[34] **7**.[35] The line shape analysis of the temperature dependent ^{1}H NMR spectra of compounds **5** and **6** was carried out according to the method described by Günther.[36] Crystal data of compound **1**: $M_r = 796.18$; triclinic; space group $P\bar{1}$; cell dimensions: $a = 10.819(2)$, $b = 17.251(3)$, $c = 18.370(5)$ Å, $\alpha = 107.31(2)$, $\beta = 102.71(2)$, $\gamma = 90.07(2)^{\circ}$; $V = 3185.1(11)$ Å^3; $D_{calc} = 1.660$ Mg cm^{-3}; $Z = 4$; $F(000) = 1568$; graphite monochromated Mo-Kα radiation

($\lambda = 0.710\,73$); $T = 293(2)$ K. Data were collected with a Nonius MACH3 diffractometer on a crystal with the dimensions $0.3 \times 0.3 \times 0.3$ mm. Data collection range: $4.0° < 2\theta < 52.0°$. Of a total of 9964 collected reflections 9964 were unique and 4662 with $I > 2\sigma(I)$ observed. Absorption correction was done with ψ-scans. The structure was solved by direct methods using SHELXS 86. In the asymmetric unit two independent molecules were found. 721 parameters were refined with all data by full matrix least squares on F^2 using SHELXL93 (G. M. Sheldrick, Göttingen, 1993). All non-hydrogen atoms were refined anisotropically. The hydrogen atoms were fixed in idealized positions using a riding model. Final *R*-values: $R1 = 0.0507$ [$(I > 2\sigma(I)$] and $wR2 = 0.1503$ (all data); largest peak (0.721 e Å^{-3}) and hole (-0.520 e Å^{-3}). Full crystallographic details, excluding structure factor tables, have been deposited at the Cambridge Crystallographic Data Centre (CCDC). For details of the deposition scheme, see 'Instructions for Authors', *J. Chem. Soc.*, *Perkin Trans. 2*, available *via* the RSC Web page (http://www.rsc.org/authors). Any request to the CCDC for this material should quote the full literature citation and the reference number 188/126.

Computational methods

For the MNDO and PM3 calculations the semiempirical molecular orbital package VAMP7.0[19] was used. All calculations were performed with the default parameters and Baker's Eigenvector Following (EF) routine described in ref. 37. The reaction coordinates were created by variation of the distance between the *ortho* C-atoms of one anisole ring and the centre of mass. For the discussion of point charges and molecular electrostatic potentials the natural atomic orbital/point charge (NAO-PC) model[38] implemented in VAMP was used. The visualisation of these properties was achieved with the program TRAMP.[39] All molecular mechanic calculations were performed with the PIMM91 force field using the default parameters and convergence criterias described in ref. 20. The point charges in the force field calculations were obtained from the geometry optimisation of the neutral molecules with the Murtagh and Sargent method.[40]

Acknowledgements

We thank Dr M. Kroeker (TU Darmstadt) for helpful discussions and for providing us with the PIMM force field program and Dr V. Böhmer for the helpful discussion. This work was supported by the Fonds der Chemischen Industrie.

References

1 C. D. Gutsche, *Calixarenes*, The Royal Society of Chemistry, Cambridge, UK, 1989.
2 *Calixarenes, A Versatile Class of Macrocyclic Compounds,* ed. J. Vicens and V. Böhmer, Kluwer, Dordrecht, 1991.
3 V. Böhmer, *Angew. Chem.*, 1995, **107**, 785.
4 S. Shinkai, *Tetrahedron*, 1993, **49**, 8933.
5 K. Iwamoto, K. Araki and S. Shinkai, *J. Org. Chem.*, 1991, **56**, 4955.
6 E. Ghidini, F. Ugozzoli, R. Ungaro, S. Harkema, A. A. El-Fadl and D. N. Reinhoudt, *J. Am. Chem. Soc.*, 1990, **112**, 6979.
7 C. D. Gutsche, B. Dhawan, A. J. Levine, K. H. No and L. J. Bauer, *Tetrahedron*, 1983, **39**, 409.
8 T. Harada, J. M. Rudzinski and S. Shinkai, *J. Chem. Soc.*, *Perkin Trans. 2*, 1992, 2109.
9 L. C. Groenen, J. D. van Loon, W. Verboom, S. Harkema, A. Casnati, R. Ungaro, A. Pochini, F. Ugozzoli and D. N. Reinhoudt, *J. Am. Chem. Soc.*, 1991, **113**, 2385.
10 S. Fischer, P. D. J. Grootenhuis, L. C. Groenen, W. P. van Hoorn, F. C. J. M. van Veggel, D. N. Reinhoudt and M. Karplus, *J. Am. Chem. Soc.*, 1995, **117**, 1611.
11 W. P. van Hoorn, *Conformational and Dynamical Properties of Calixarenes*, Proefschrift, University of Twente, 1997, and references cited therein.
12 J. C. van Loon, L. C. Groenen, S. S. Wijmenga, W. Verboom and D. N. Reinhoudt, *J. Am. Chem. Soc.*, 1991, **113**, 2378.
13 J. Blixt and C. Detellier, *J. Am. Chem. Soc.*, 1994, **116**, 11 957.
14 P. D. J. Grootenhuis, P. A. Kollman, L. C. Groenen, D. N. Reinhoudt, G. J. van Hummel, F. Ugozzoli and G. Andreetti, *J. Am. Chem. Soc.*, 1990, **112**, 4165.
15 A. Arduini, M. Fabbi, M. Mantovani, L. Mirone, A. Pochini, A. Secchi and R. Ungaro, *J. Org. Chem.*, 1995, **60**, 1454.
16 M. Conner, V. Janout and S. L. Regen, *J. Am. Chem. Soc.*, 1991, **113**, 9670.
17 A. Ikeda, H. Tsuzuki and S. Shinkai, *J. Chem. Soc.*, *Perkin Trans. 2*, 1994, 2073.
18 For our semiempirical calculations we used the VAMP program package: G. Rauhut, A. Alex, J. Chandrasekhar, T. Steinke, W. Sauer, B. Beck, M. Hutter, P. Gedeck and T. Clark, VAMP7.0, Oxford Molecular Ltd., Madawar Centre, Oxford Science Park, Standford-on-Thames, Oxford, OX4 4GA, UK, 1996; (*a*) MNDO: J. S. Dewar and W. Thiel, *J. Am. Chem. Soc.*, 1977, **99**, 4899; (*b*) PM3: J. J. Stewart, *J. Comput. Chem.*, 1989, **10**, 209; 221.
19 PIMM: H. J. Lindner, *Tetrahedron*, 1972, **30**, 1127; A. E. Smith and H. J. Lindner, *J. Comput.-Aided Mol. Des.*, 1991, **5**, 235; M. Kroeker, PhD Thesis, Technische Hochschule, Darmstadt, 1994.
20 Notation introduced by Reinhoudt and co-workers.[10] The numbers denote the anisole units whereby 0 accounts for a non inverted anisole ring and 1 accounts for an inverted one. The letters A and B mark the position of the methoxy group attached to the corresponding benzene ring. A denotes a methoxy group pointing outward and B denotes a methoxy group pointing inward the cavity.
21 F. A. Bovey, *Nuclear Magnetic Resonance Spectroscopy*, Academic Press, New York and London, 1969, pp. 61–71, 264–274.
22 We used the PM3 structure as a model because its higher symmetry facilitates such qualitative geometrical considerations.
23 Values taken from ref. 11.
24 For the equilibrium (2) $\Delta H = -9.8$ kcal mol^{-1} was calculated.[11]
25 I. Thondorf, J. Brenn, W. Brandt and V. Böhmer, *Tetrahedron Lett.*, 1995, **36**, 6665.
26 G. D. Andreetti, V. Böhmer, J. G. Jordan, M. Tabatabai, F. Ugozzoli, W. Vogt and A. Wolff, *J. Org. Chem.*, 1993, **58**, 4023.
27 J. Scheerder, R. H. Vreekamp, J. F. J. Engbersen, W. Verboom, J. P. M. van Duynhoven and D. N. Reinhoudt, *J. Org. Chem.*, 1996, **61**, 3476.
28 For the 25,26,27,28-tetraoctyloxycalix[4]arene Arduini *et al.*[15] found $\Delta G^{\ddagger} = 10.2$ kcal mol^{-1}. The introduction of four COOH or four CONH$_2$ groups in the upper rim increases $\Delta G^{\ddagger}$ due to intramolecular H-bonding to 14.1 and 13.3 kcal mol^{-1} respectively.[16] Böhmer and co-workers[26] reported a $\Delta G^{\ddagger}$ of 13.3 kcal mol^{-1} for the C_2/C_2 interconversion in a dissymetric calix[4]arene.
29 This value is similar to the $\Delta S^{\ddagger}$ of -3.8 cal mol^{-1} K^{-1} for the *paco*-**4**/*cone*-**4** conversion determined by Blixt and Detellier,[13] and should be compared with $\Delta S^{\ddagger} = -R \ln 4 = -2.8$ cal mol^{-1} K^{-1} accounting for the changes in the symmetry numbers of those species.
30 Obviously the PM3 method is inappropriate to quantitatively reproduce the experimental results. However it has to be considered that 0 K structures in the gas phase neglecting all solvent interactions are considered. Better agreement with experimental results was achieved with force field calculations.[10,11].
31 This value is comparable with $\Delta S^{\ddagger} = -16.7$ cal mol^{-1} K^{-1} for the **4**-*paco*/**4**-1,2-*alt* conversion.[13]
32 C. D. Gutsche and P. F. Pagoria, *J. Org. Chem.*, 1985, **50**, 5795.
33 W. Verboom, A. Durie, R. J. M. Egberink, Z. Asfari and D. N. Reinhoudt, *J. Org. Chem.*, 1992, **57**, 1313.
34 R. A. Jakobi, V. Böhmer, C. Grüttner, D. Kraft and W. Vogt, *New J. Chem.*, 1996, **20**, 493.
35 I. Bitter, A. Grün, B. Ágai and L. Tôke, *Tetrahedron*, 1995, **51**, 7835.
36 H. Günther, *NMR-Spektroskopie*, Georg Thieme Verlag, Stuttgart, New York, ch. 9, 1992.
37 J. Baker, *J. Comput. Chem.*, 1986, **7**, 385.
38 G. Rauhut and T. Clark, *J. Comput. Chem.*, 1993, **14**, 503.
39 TRAMP 1.1b, H. Lanig, R. Koenig and T. Clark, Erlangen, 1995.
40 B. A. Murtagh and R. W. H. Sargent, *Comput. J.*, 1970, **13**, 185.

Paper 7/08606G
Received 28*th November* 1997
Accepted 13*th March* 1998